COVER SHEET

NOTE: This coversheet is intended for you to list your article title and author(s) name only —this page will not appear on the Electronic Product.

Title: *Investigating transverse ply thickness and cracking effects on the tensile strain to failure of thin-ply, cross-ply carbon composites using X-ray computed tomography*

Authors: Tamas Rev
Frank A. Leone,
Andrew E. Lovejoy and
Michael R. Wisnom

PAPER DEADLINE: ****See Editor****

PAPER LENGTH: ****See Editor****

SUBMISSION PROCEDURE: **Information on the electronic submission of manuscripts is provided on the conference web site.**

INQUIRIES TO: **See Editor**

We encourage you to read attached Guidelines prior to preparing your paper—this will ensure your paper is consistent with the format of the articles in the Electronic product.

NOTE: Please submit your paper in Microsoft Word® format or PDF if prepared in a program other than MSWord. Sample guidelines are shown with the correct margins. Follow the style from these guidelines for your page format.

Electronic file submission: When making your final PDF for submission make sure the box at "Printed Optimized PDF" is checked. Also—in Distiller—make certain all fonts are embedded in the document before making the final PDF.

(FIRST PAGE OF ARTICLE)

ABSTRACT

The effect of 90°-ply thickness on the fibre direction tensile failure strain of cross-ply laminates was investigated by designing four different cross-ply composite laminate configurations with 90° blocks of varying numbers of plies adjacent to a central block of 0° plies. The range of 90° block thicknesses evaluated included conventional ply thicknesses to allow for comparisons with conventional ply geometries. The central 0° ply block was subjected to primarily longitudinal tension with a small component of transverse tension due to the layup and thermal residual stresses. Advanced instrumentation, including acoustic emission and X-ray computed tomography, was used to detect and visualize damage accumulation in the specimens. It was found that decreasing the thickness of the 90° ply blocks reduced transverse matrix microcracking up to the point where no full-width transverse cracks developed prior to ultimate failure. A small degradation of the fibre direction failure strain in the central 0° plies was found as the 90°-layer thickness increased in the laminates, which corresponded with the development of edge/transverse cracks.

Tamas Rev, Bristol Composites Institute (ACCIS), University of Bristol, Queens Building, University Walk, Bristol, BS8 1TR, UK,
Michael R. Wisnom, Bristol Composites Institute (ACCIS), University of Bristol, Queens Building, University Walk, Bristol, BS8 1TR, UK,
Frank A. Leone, NASA Langley Research Center, Hampton, VA 23681, USA,
Andrew E. Lovejoy, NASA Langley Research Center, Hampton, VA 23681, USA.

INTRODUCTION

The use of thin-ply composite materials continues to grow significantly in key industries such as aircraft and space, in part due to higher potential laminate strengths and the suppression of microcracking in thin-ply layers. One of the key challenges to accurately model and predict the failure of such materials is the difficulty in generating reliable experimental data that can be compared with predictions [1]. This is especially true for multi-axial and combined loadings that resemble real-life operating conditions and there is a lack of good data to help validate the predictions of the response of such fibrous materials [2]. Even for unidirectional (UD) laminates, accurately determining their fundamental mechanical properties such as failure strain or strength is still a scientific challenge. For instance, the experimental strength measurements of UD carbon/epoxy composites can be affected by stress concentrations at the end-tab regions of the specimens in tensile tests. A significant knock-down in their measured strengths may be observed, premature failure can occur, and notably lower strains than expected from the failure strain of the fibres can be measured [3].

This study aims to look at the effect of 90°-ply thickness on the failure mode and strain of cross-ply laminates under longitudinal tension and determine whether thin-ply composites can suppress transverse micro-cracking away from the edges. Hybrid specimens are designed in which the so-called hybrid effect and the in-situ (thickness) effect are considered. The hybrid effect in this case is an apparent failure strain enhancement: in a thin-ply interlaminar hybrid configuration which consists of, e.g., standard-thickness glass and thin carbon composite layers, the failure strain of the carbon layers would be higher than the failure strain of the carbon in a non-hybrid configuration due to constraint from the glass layers on forming a critical cluster of broken carbon fibres. This hybrid effect can result in an increased failure strain for very thin plies and is different from the expected strain enhancement due to the size effect. The magnitude of the size effect is relatively small and is in addition to the failure strain enhancement due to the hybrid effect, as demonstrated previously by Wisnom et al [4].

As transverse matrix cracking is one of the most common damage mechanisms associated with cross-ply laminates [5], its effect on the measured longitudinal failure strain of the material is investigated by changing the 90° ply thickness to alter the degree of cracking and overall extent of matrix damage prior to fiber failure.

MATERIAL, DESIGN AND CONFIGURATION

Material

The materials used in the experimental specimens were a thin-ply TC33 carbon fibre prepreg (Formosa Plastics) supplied by SK Chemicals and a standard ply S-Glass fibre material supplied by Hexcel. Both epoxy resin systems were 125 °C cure polymers. The matrix for the glass fibre was a 913-epoxy from Hexcel and a K51 epoxy resin system by Skyflex was used for the carbon. Basic properties of the applied fibre and prepreg systems can be found in Table I and Table II, respectively. The fibre volume fraction of the carbon prepreg is significantly lower than typical values for standard-thickness plies (approximately 60%).

TABLE I. FIBRE PROPERTIES OF THE UNIDIRECTIONAL PREPREGS BASED ON MANUFACTURERS DATA

Fibre type	Elastic modulus [GPa]	Density [g/cm^3]	Strain to failure [%]	Tensile strength [GPa]
Tairyfil TC33 carbon [6]	230	1.8	1.5	3.45
FliteStrand SZT S-Glass [3]	88	2.45	5.5	4.8-5.1

TABLE II. CURED PLY PROPERTIES OF THE UNIDIRECTIONAL PREPREGS

Prepreg type	Areal density [g/m^2]	Cured ply thickness [μm]	Fibre volume fraction [%]	Initial elastic modulus [GPa]	Tensile strain to failure [%]
TC33/K51 carbon/epoxy[1]	21	30	39	95.3	1.61
S-Glass/913 glass/epoxy [2]	190	155	51	45.7	3.98

[1]Based on measurements
[2]Based on measurements from [3]

Design and configurations

The design of the specimens involved two key considerations: the hybrid effect [4] and the thickness effect [7]. The hybrid effect can result in an increased fiber failure strain for very thin plies as demonstrated previously by Wisnom *et al.* [4]. Consequently, a central 0° ply thickness of 0.12 mm (four plies of TC33/K51 material) was chosen as the basis of the configurations to avoid the hybrid effect and better isolate the thickness effects. To investigate thickness effects (also referred to in the literature as the in-situ effect) on transverse cracking, configurations needed to be designed in a way that allows for varying the number of 90° plies while maintaining the same overall stress state and stiffness of the laminates where possible. A structure of [$Y/X/90_n/0_4/90_n/X/Y$] was proposed where the central zero ply block (0_4) is surrounded by 90_n blocks where n = 1, 2, 4, and 8. The outer part of the laminates (referred to as X) consisted of only 0° and 90° plies with the same total number of plies of each orientation in order to keep the overall stiffness consistent for each configuration. The ply orientations were alternated to minimize the likelihood for cracking in these plies.

Additionally, glass layers (referred to as Y) were incorporated on the surface of the laminates in order to avoid the stress concentrations arising at the grips during static tensile testing and to acquire repeatable and consistent results with clear gauge section failures of the specimens. This approach follows Czél *et al.* [3], who found significantly higher failure strains were obtained with surface glass layers than from conventional non-hybrid carbon/epoxy baseline specimens. This eliminated the need for optimising the gripping conditions of the tensile specimens. The glass layer thicknesses were calculated according to the design formulas developed by Czél *et al.* in order to ensure that the glass layers can still carry the load after the failure of the carbon composite. An illustration of a typical specimen comprising the thin-ply carbon/epoxy cross-ply laminate, its structure and the embedding protective glass layers is shown in Figure 1.

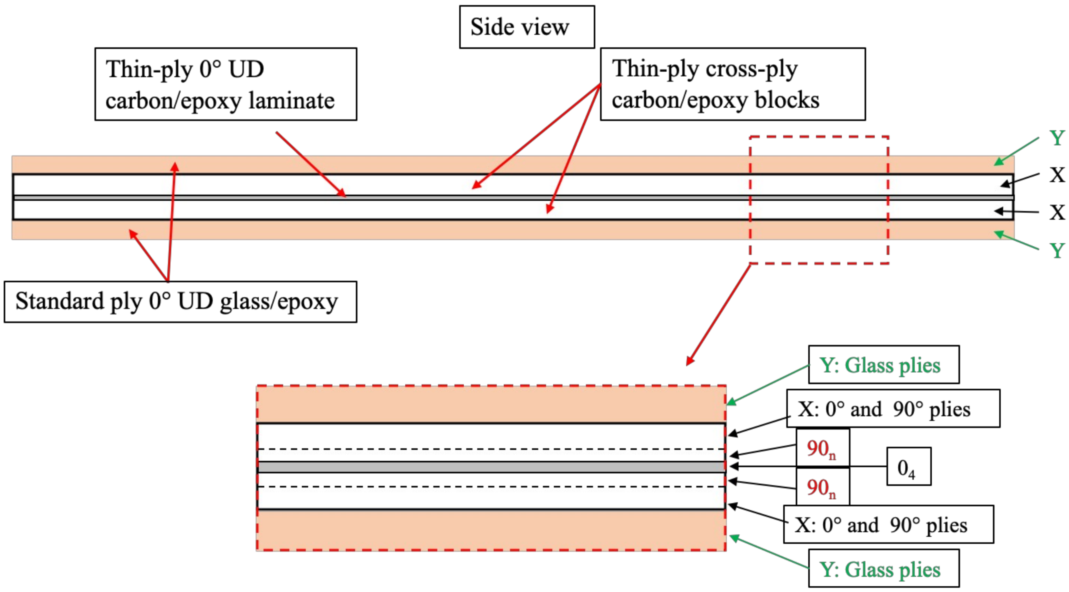

Figure 1. Schematic of a typical cross-ply laminate configuration: thin-ply UD carbon/epoxy is surrounded by blocks of thin-ply cross-ply carbon blocks, embedded in standard thickness UD glass/ epoxy ply blocks.

A summary of the four different lay-ups designed using Classical Laminate Analysis (CLA) can be found in Table III. The green colour represents the embedding glass layers, while the red represents the 90_n blocks with varying number of plies adjacent to the central 0° layers.

To determine the stacking sequence of the outer 0° and 90° blocks (marked with X), first, the 90° and 0° plies were placed as single layers as many times as needed to reach a total of 28 plies for each laminate (to be consistent with other studies by the first author). Then, as the 90_n block adjacent to the central 0_4 ply block increased in thickness, some of the 90° plies in X were placed in a different position and the 0° plies adjacent to the 90° plies were blocked.

For the first three configurations of 90_n blocks with n = 1, 2, 4, the total number of adjacent 0° and 90° plies were kept the same. However, for the configuration with 8 blocked 90° plies adjacent to the central 0° layers, it was not possible to keep the stiffness ratio constant as there was an excess number of 90° plies within the laminate. Hence, this configuration had a slightly higher stiffness when compared to the others.

The following properties were used for the carbon in the analysis: E_{11} = 95.3 GPa, E_{22} = 6.11 GPa, G_{12} = 2.47 GPa, ν_{12} = 0.3, $\alpha_1 = -1\times10^{-6}$ [1/K] and $\alpha_2 = 4\times10^{-5}$ [1/K]. Table III also includes the nominal longitudinal and transverse stresses calculated in the central 0° plies at an estimated strain to failure of ε = 1.61%. The transverse thermal residual stresses in the central 0° plies were calculated to be 16 MPa for configuration 1 to 3 and 19 MPa for configuration 4, respectively, and are incorporated in the transverse stresses (σ_y) in Table III below. Shear stresses are zero in all configurations, away from the edges.

TABLE III. LAMINATE LAY-UPS FOR TYPES 1-4 SPECIMENS: GREEN COLOUR REPRESENTS THE EMBEDDING GLASS LAYERS, WHILE THE RED REPRESENTS THE 90_n BLOCKS. STRESSES ARE PRESENTED AT EXPECTED FAILURE STRAIN.

		Stress in central 0° plies		
	Configuration	σ_y/σ_x [-]	σ_x [MPa]	σ_y [MPa]
1.	**$[0_6/(0/90)_5/0/90/0_2]_s$**	0.023	1522	35
2.	**$[0_6/0_2/90/(0/90)_3/0/90_2/0_2]_s$**	0.023	1522	35
3.	**$[0_6/0_2/90/0_2/90/0_2/90_4/0_2]_s$**	0.023	1522	35
4.	**$[0_6/0_2/90/0_2/90/0_2/90_8/0_2]_s$**	0.026	1518	40

EXPERIMENTS

Specimen manufacturing and geometry

The specimens tested in this study were parallel edge tensile specimens as outlined in Figure 1. The nominal dimensions for all cross-ply coupons (Type 1-3) were 270/190/20/2.70 mm overall length/gauge length/width/thickness, respectively. Type 4 specimens had the same nominal dimensions except in the thickness direction, which had a nominal value of t = 2.94 mm. Seven coupons were tested for each configuration.

The fabrication of the composite laminates involved a hand lay-up followed by an autoclave consolidation procedure using a vacuum bagging method on a flat aluminium tool plate. The cure cycle used was 60 minutes at 80°C and 100 minutes at 125°C with 0.7 MPa applied pressure and a heat up and cool down rate of 2°C/min. In the finishing stage, the specimens were cut to the desired nominal geometry specified above using a CNC controlled diamond particle coated cutting wheel. After that, each end of the specimens was hand-sanded using Grit P120 polishing paper in order to increase the surface roughness of the composites at the gripped sections (40 mm at each end).

Test method

Uniaxial tensile tests were carried out in accordance with the ASTM D3039 standard [8] on an Instron 8801 universal servo-hydraulic mechanical testing machine. The machine was equipped with a 100 kN rated load cell and hydraulic wedge grips. The grips were 50 mm wide Instron 2704-521 type serrated steel jaw faces. Loading was introduced under displacement control at a crosshead speed of 2 mm/min. Clamping pressure was kept as low as possible, but sufficient to avoid slippage of the coupons.

The strain measurement was carried out using a 2D Imetrum video gauge system (based on digital image correlation principles) [9] outputting the corresponding force, time, and strain data. Strains are measured over the gauge section area of the specimens.

Additionally, a PCI-2 acoustic emission (AE) system was used to identify damage events during the loading process. The AE sensors were PAC WSA type, broadband, piezoelectric transducers with a frequency range of 100-1000 kHz. The maximum sampling rate was 40 MHz and the gain selector of the preamplifier and threshold value were set to 40 dB.

Seven replicates were tested until failure for each configuration using video gauge strain measurements and AE. Additionally, interrupted tests were also conducted to document the development and progression of matrix cracks in the different configurations. These results were used to enable study and assessment of the effect of transverse matrix cracking on the longitudinal failure strain as described later.

To verify such damage events (transverse matrix cracking) and compare with the ones detected by AE, an in-situ testing rig developed at NASA by Matheson [10] was used to carry out in-situ X-Ray scans of the designed configurations. An illustration of the test fixture is shown in Figure 2.

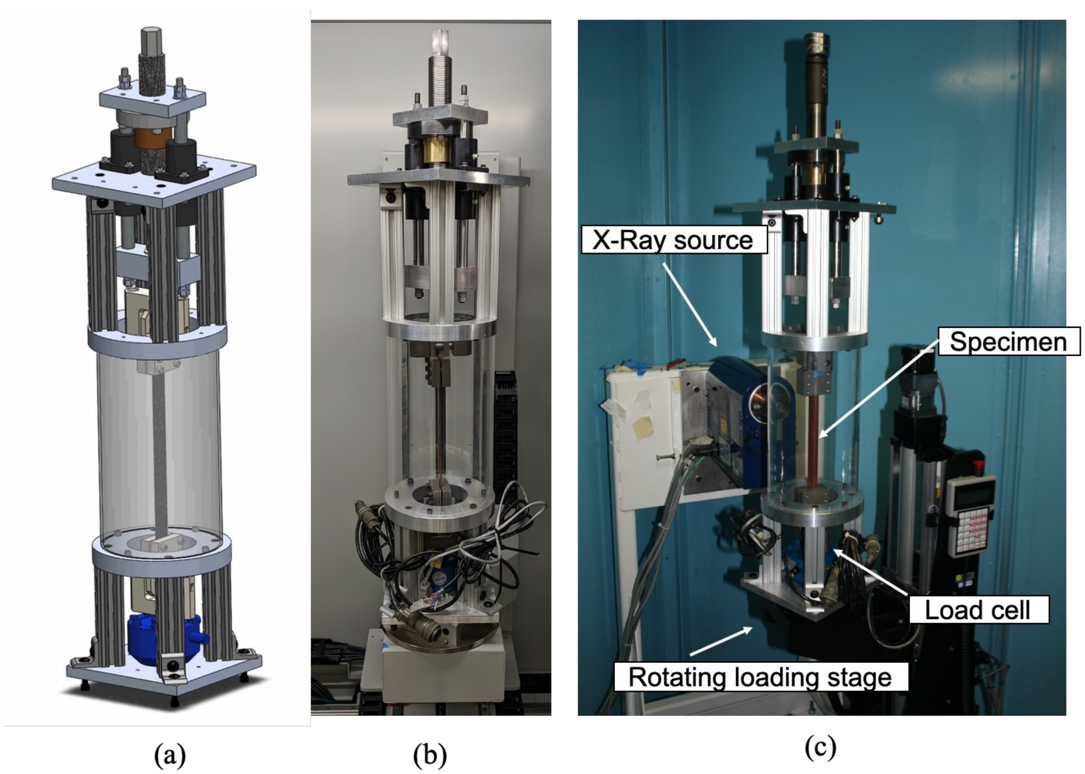

Figure 2. In-situ test fixture (a) design drawing reproduced from Matheson [10], (b) test fixture at the NASA Langley Research Center, and (c) testing rig integrated to the rotating stage in the X-ray CT system at NASA.

The main objective was to execute interrupted tests in order to detect the existence and record the onset and extent of cracking in the presented laminate configurations at increasing load levels. Another objective was to determine the effect of 90°-layer thickness on the cracking strain of the material. Exploratory tests were carried out to set up the fixture for tensile load application and to develop an efficient method for loading and scanning the specimens to highlight the desired damage. This ensured that testing parameters were consistent for all tests and specimens, and the results are comparable.

After initial tests it was found that simply using an in-situ X-ray CT test was not sufficient to highlight cracking occurring in such thin-ply specimens. Consequently, an 'ex-situ' X-ray CT procedure was developed that proved successful in showing the damage state of the specimens. The procedure consisted of the following steps: (i) the specimen was loaded to a set percentage of peak load level to generate damage within the coupon, (ii) the specimen was unloaded, (iii) dye penetrant was applied with a syringe on the edge of the specimens (iv) the specimen was loaded up to a nominal load of ≈ 24.5 kN (60% of average peak failure load) to open up any cracks present (v) dye penetrant was applied again on the edge of the specimens so that it could infiltrate/ penetrate the cracks through capillary action, (vi) the specimen was unloaded and an X-ray CT scan was performed. The double application of dye penetrant was carried out only to make sure the dye penetrated all the cracks possible; however, it was not necessary. The dye penetrant used was a zinc iodide solution that contained ZnI_2 powder, water, isopropyl alcohol, and Kodak Photo Flo type wetting agent. The scanned area of the specimens was 35 x 20 mm with a resolution of 17.6 microns per voxel. The images disclosed represent all damage within the carbon layers.

The X-ray CT system was manufactured by HYTEC, Inc. The X-ray CT system consists of a Varian PaxScan 4030E detector with 2300 x 3200 pixels resolution and Kevex 130kV microfocus source. X-Ray settings ranged from 100 to 115 kV with the current being set in the range of 100 to 115 mA. The X-ray CT system has a rotating loading stage where the in-situ testing rig was purpose designed to fit and rotate while the stationary X-Ray source was in operation. An average of 1700 images per scan were taken (1700 steps in the 360-degree rotation of the specimen). Each image had a capture time of 1 second. For the reconstruction and viewing of the images, the commercially available software VG Studio Max from Volume Graphics was used.

Results and discussion

MECHANICAL TESTING

The stress- strain response of the four different configurations tested are presented in Figure 3. The curves correspond to loading up to the ultimate failure of the cross-ply carbon laminate within the glass layers. Plotting of the graphs was stopped at the point of the load drop corresponding to carbon fracture.

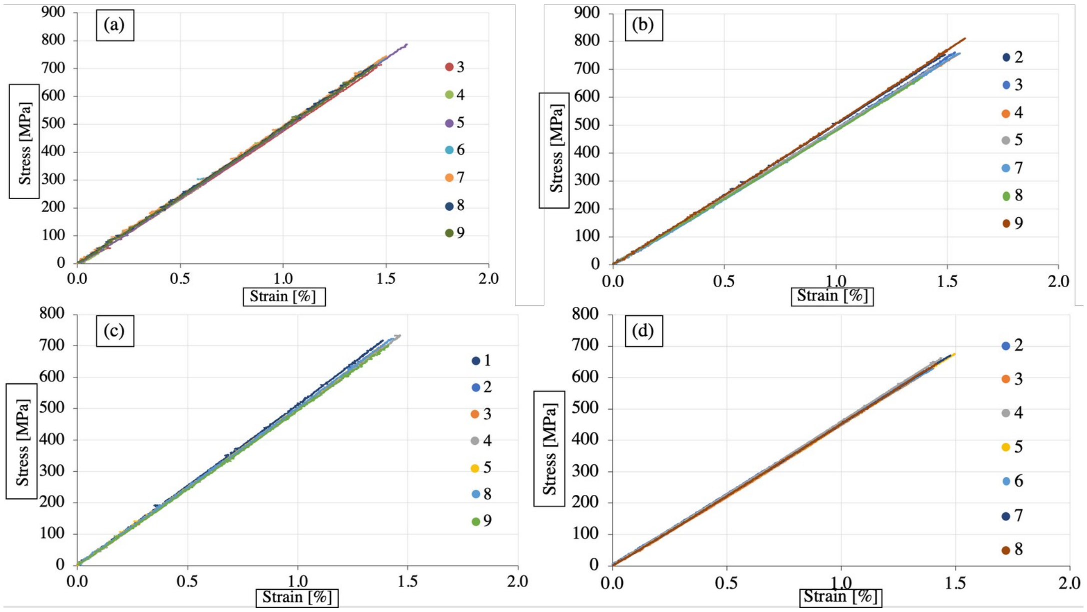

Figure 3. Stress – strain responses acquired during mechanical testing of the designed (a) Type 1, (b) Type 2, (c) Type 3 and (d) Type 4 configurations respectively.

A slight tension stiffening can also be observed in the response of all configurations. The measured failure load at the drop, longitudinal and transverse direction strains at load drop and the calculated net section stresses for the whole laminate (including the glass layers) at the load drop are shown in Table IV. All the acquired data in Table IV are average values with the corresponding number of coupons tested and their respective variability (coefficient of variation [%]). The baseline measurements are reported in [6] where SG_2 denotes two layers of S-Glass prepreg material.

TABLE IV. SUMMARY OF THE MECHANICAL MEASUREMENTS AND ESTIMATED STRESSES FOR THE CROSS-PLY CONFIGURATIONS

	Configuration	No. of spec. tested [-]	Drop load P [kN] (CoV%)	Long. strain at load drop ε_{xx} [%] (CoV %)	Trans. strain at load drop ε_{yy} [%] (CoV %)	Stress at load drop σ_{xx} [MPa] (CoV%)
	Baseline $[SG_2/0_2]_s$	8	13.8 (3.2)	1.65 (3.0)	-0.50 (5.0)	900 (3.7)
1.	**$[0_6/(0/90)_5/0/90/0_2]_s$**	7	41.1 (5.2)	1.50 (4.5)	-0.20 (10.0)	732.8 (4.7)
2.	**$[0_6/0_2/90/(0/90)_3/0/90_2/0_2]_s$**	7	41.6 (4.7)	1.51 (4.6)	-0.21 (10.1)	746.6 (4.7)
3.	**$[0_6/0_2/90/0_2/90/0_2/90_4/0_2]_s$**	7	39.5 (1.4)	1.41 (3.0)	-0.20 (5.1)	708.9 (2.5)
4.	**$[0_6/0_2/90/0_2/90/0_2/90_8/0_2]_s$**	7	39.0 (2.6)	1.43 (3.3)	-0.15 (8.2)	646.9 (3.4)

ACOUSTIC EMISSION MEASUREMENTS

Representative cumulative energy curves acquired are presented in Figure 4. Types 1-3 specimens do not show a rise in cumulative energy until the failure of the carbon block. However, for Type 4 specimens, damage events appear earlier during loading which is indicated by the rise in the cumulative energy prior to failure. These observations give an indication of damage, but further investigation was carried out to determine the true damage state of the specimens.

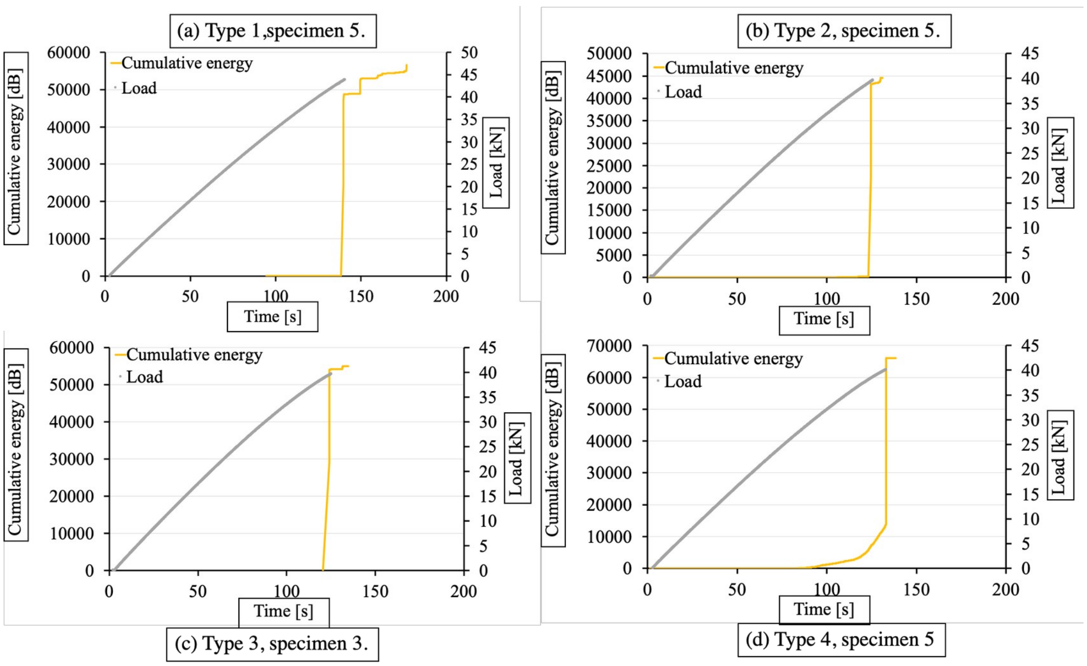

Figure 4. The cumulative energy measured during testing of the different type configurations: (a) Type 1 (b) Type 2 (c) Type 3 and (d) Type 4 respectively.

X-RAY CT MEASUREMENTS

Initially, in-situ X-ray CT tests were carried out to assess the damage state and the presence of cracks in the different configurations. These tests involved taking an intact specimen and loading it using the in-situ fixture shown in Figure 2 to a specific load level in order to open up the cracks within the laminate and then conducting X-Ray CT examination.

For Type 1 and Type 2 specimens with 90_1 and 90_2 layers adjacent to the central 0° block, transverse cracking within the 90 layers was not expected due to the low layer thickness. However, for the Type 3 and Type 4 coupons with blocks of 90_4 and 90_8 plies adjacent to the central zeroes, the appearance of transverse cracks was more likely due to the increased layer thickness.

The percentage load levels defined for the ex-situ scans were appropriate to the configuration: for the Type 1 and Type 2 specimens it was desirable to achieve the highest load level possible as cracking was not expected, whilst for Type 3 and Type 4 coupons it was desirable to reduce the load level to be able to determine the onset of first cracking. In some cases (Type 1 and Type 2 configuration) higher load levels could not be achieved for the interrupted tests due to the premature failure of the specimens. The test matrix with the load levels acquired for the interrupted tests for each configuration is shown in Table V.

TABLE V. SUMMARY OF TEST MATRIX FOR THE INTERRUPTED X-CT TESTS

Configuration	Drop load P [kN] (CoV%)	Load levels for interrupted tests [%] (Equivalent load in [kN])				
1. **[0_6/(0/90)$_5$/0/90/0_2]$_s$**	41.1 (5.2)	89.0 (36.6)	86.7 (35.6)	84.5 (34.7)	-	-
2. **[0_6/0_2/90/(0/90)$_3$/0/90_2/0_2]$_s$**	41.6 (4.7)	92.7 (38.6)	-	85.0 (35.4)	-	-
3. **[0_6/0_2/90/0_2/90/0_2/90_4/0_2]$_s$**	39.5 (1.4)	95.9 (37.9)	90.1 (35.6)	85.0 (33.6)	80.0 (31.6)	70.0 (27.7)
4. **[0_6/0_2/90/0_2/90/0_2/90_8/0_2]$_s$**	39.0 (2.6)	95.9 (37.4)	-	83.9 (32.7)	80.0 (31.2)	70.0 (27.3)

Overall, the X-Ray images taken for all configurations exhibited some form of damage due to material defects. Generally, there were no transverse cracks observed in the outer 90° plies (either single or double block) but only in the thicker plies adjacent to the central 0° layer. The failure of the laminates was indeed only influenced by the 90° block adjacent to the central 0° layer. There were no full width transverse cracks found in the Type 1, Type 2 or Type 3 laminates. However with the 90_8 block, for the Type 4 coupons, full width transverse cracks appeared as well.

The damage mechanism in thin-ply laminates differs from that of the thicker ones: for thin-ply composites, damage may initiate at low stress levels but that does not necessarily lead to the final failure of the laminate. Crack propagation is mostly energy driven, and so for thin layers, if a crack were to develop within the layer, it would not have enough energy to propagate. Hence, for thin plies some localized edge cracks might initiate, however, there is not enough energy to propagate to a full width transverse crack. This was the case for the Type 1-3 specimens. An illustration of that is found in Figure 5, where X-ray CT images taken of a Type 2 specimen interrupted at (a) 85% and (b) 92% of the peak failure load are shown. The images show a damage pattern similar to the Type 1 specimens: inherent material defects as well as some free edge cracks that do not extend across the width of the specimen.

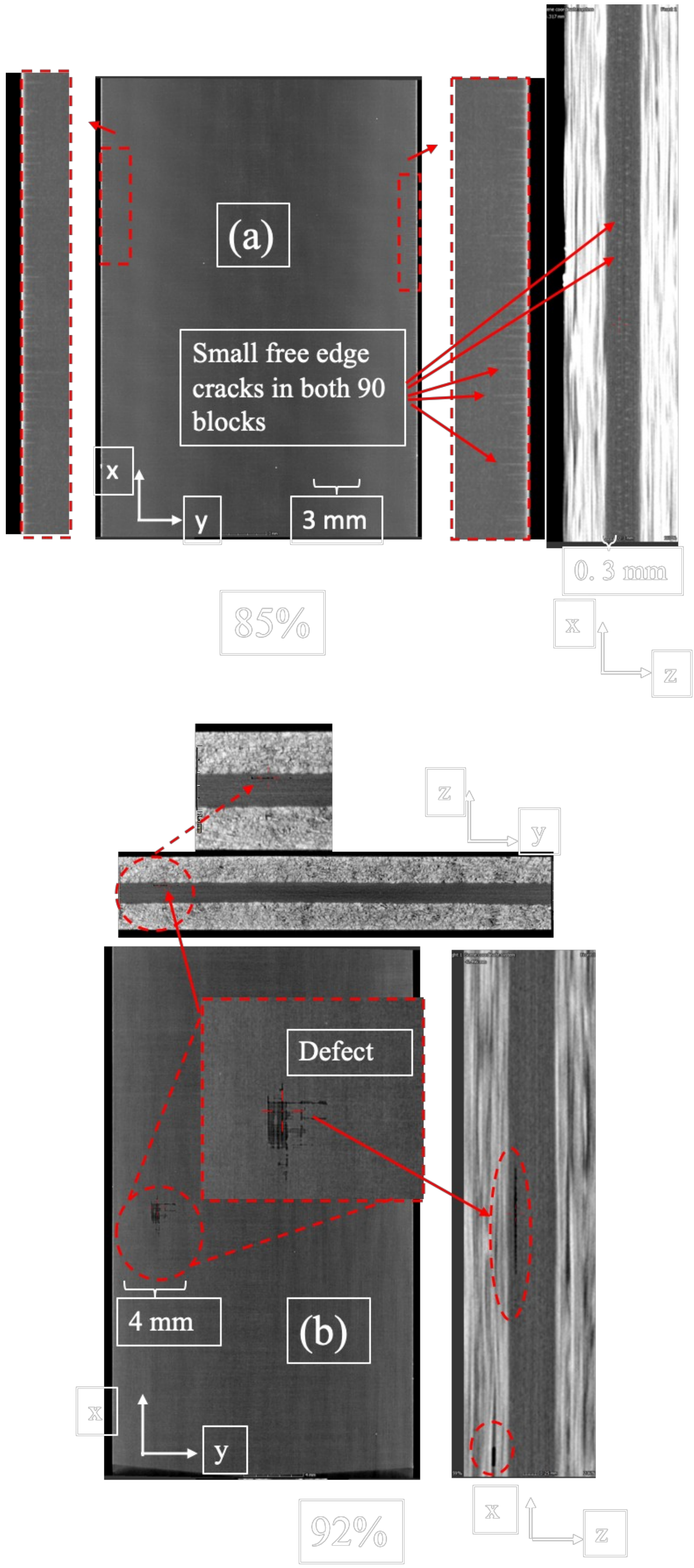

Figure 5. X-ray CT images taken of Type 2 specimens interrupted at (a) 85% and (b) 92% of the peak failure load. The images show a similar damage pattern to the Type 1 specimens due to inherent material defects as well as some free edge cracks that do not extend across the width of the specimen.

Transverse crack initiation is dependent on clusters of fibres, weak points, local stress concentrations, defects, voids, etc., and once a critical stress level is reached, individual cracks may propagate instantaneously through the thickness and width direction if the ply is thick enough (Type 4 configuration). An illustration of some cracks extending across the width of the laminate is shown in Figure 6. All images were taken in the center of the 90-block adjacent to the central 0° plies, and the observed length of the cracks does not change through the thickness of the 90 blocks. The red arrow indicates an increase in the crack length and density as the load level increases.

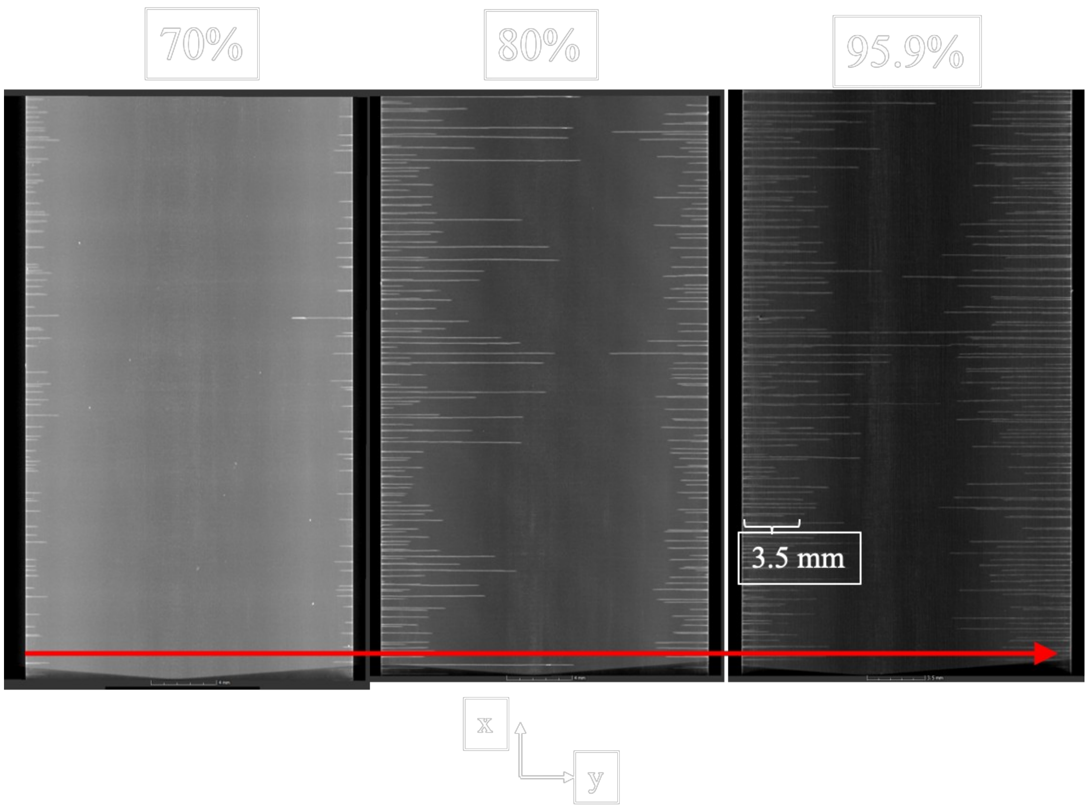

Figure 6. X-ray CT scans of the interrupted Type 4 specimens at three different load levels – 70%, 80% and 95.9% of the peak failure load respectively, exhibiting some transverse cracks across the width of the laminates within the thick 90° blocks adjacent to the zeroes. The crack length and density increase as the load level increases.

Generally, the free-edge cracks and the full-width transverse cracks observed can be differentiated as separate mechanisms when defining the onset of damage in thin-ply, cross-ply laminates. This behaviour was also investigated for thin-ply composites with a varying 90° ply thickness from 300 μm down to 30 μm by Kohler et al. [11] who observed a similar behaviour where edge cracks and full width transverse cracks were considered as separate mechanisms with different onset stresses. They concluded that the propagation of edge cracks into the bulk was specific to layer thicknesses between 50 μm to 200 μm. AE measurements picked up damage events only when the edge cracks propagated into the bulk of the specimens. This was also illustrated in this study in the Type 4 specimens where extensive transverse cracking (propagating from the edge into the bulk, across the width) was picked up by the AE measurements. This observation is an inference made via correlation among experimental data from multiple specimens.

This study provides further evidence that free-edge cracks alone are not a reliable indicator of imminent failure for structures comprising thin-ply laminates. The dominant damage mechanism affecting the failure strain of the laminates is the propagation of such edge cracks into the bulk of the specimens, which can be experimentally determined through AE measurements and X-ray CT examination.

DISCUSSION

An illustration of the measured longitudinal failure strain as a function of the 90_n block thickness for all configurations including the baseline measurements without any 90 plies is shown in Figure 7.

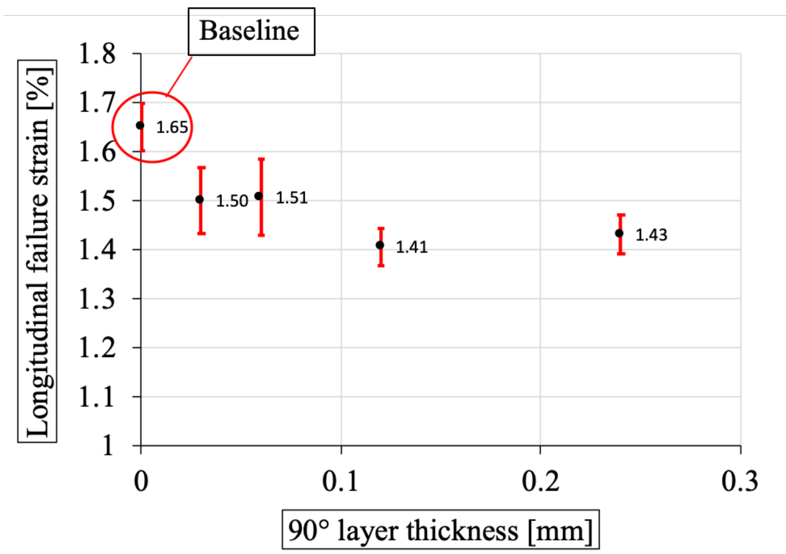

Figure 7. Measured longitudinal failure strain for the baseline specimen and all Type 1-4 specimens as a function of the interior 90°-layer thickness.

As can be seen from Figure 7, there is about 8% reduction in strain from the baseline measurements of the UD material to the configuration with single (n = 1) and double (n = 2) 90_n layers. This reduction in strain is likely to be due to the early development of free-edge cracks in the 90° plies in the Type 1 and 2 configurations when loaded in tension. Residual thermal stresses could have also contributed to the initiation of such free edge cracks. When specimens are loaded, the 0° plies experience stress concentrations imposed on them due to the free edge cracks appearing in the 90° plies. If there were no edge cracks appearing, the stress distribution in the 0° plies would be more uniform and at a lower level.

A study carried out by Xu et al. [12] looking at the effects of transverse cracking on un-notched and notched strengths of quasi-isotropic (QI) carbon/epoxy laminates showed that in a typical unnotched QI carbon/epoxy laminate with no damage present, the 90° ply experiences an increase in stress at the free edges. This increased stress state (or the extra strain present in the 90°layers) could have led to the initiation of such small free-edge cracks early on. For the Type 3 and Type 4 configurations with larger 90° block thickness, we can see a further decrease in the strain to failure in Table IV. This decrease is believed to be due to the free-edge cracks extending into the bulk of the specimens - in the case of Type 4 coupons all the way across the width - affecting a larger volume of the material.

Generally, as the block thickness increases, there is additional loading put on the 0° plies due to the presence of the extended edge cracks (Type 1-3 specimens) and/or transverse cracks (Type 4 specimens) which led to the further decrease in the fibre direction failure strain. There are two factors that may contribute to this.

On one hand, there are free edge effects, and the onset of edge cracks causes stress concentrations near the edges of the laminate. These stress concentrations can lead to the redistribution of load from 90° plies onto the adjacent 0° plies. This effect is also illustrated by the study of Xu et al. [12] who carried out FE simulations on a slice of a quasi-isotropic IM7/8552 laminate with a layup of $[45/90/\text{-}45/0]_{4s}$, with full cracks in all the 90° layers and boundary conditions representing a repeating array of cracks. This showed the effect of the special state of stress near the free edge, but since only one element was used per ply, it was insufficient to model the localized stress concentration due to the crack. The analysis showed about 5 % increase in stresses at the edges in the 0° plies when compared to the mid-section stresses [12]. On the other hand, the 0° plies locally are also affected by the stress concentrations arising ahead of the crack tips when transverse cracks develop in the bulk of the laminate.

In a modeling study by Melkinov et al. [13], the presence of transverse cracks in cross-ply laminates resulted in a drop in predicted strength of 0° plies. Their models found a 3.9 % decrease in strength for thin-ply cross-ply laminates when compared to the UD composite strength, assuming a single crack in the laminate. For the calculations, a fibre break model was used accounting for strain non-uniformity and stress concentrations induced by the transverse cracks. The stress concentrations generated around the crack tips in the model were distinct for thick and thin plies due to the difference in their opening displacements.

The models are not directly comparable with the experimental results presented here because the materials and layups are different, but they do give a qualitative indication of the potential effect. Overall, it can be said that both effects mentioned above – stress concentrations imposed locally on the 0° plies and free edge effects – are present in this study and would be expected to affect the strength of the laminates. The measured failure strain reductions in the experiments are relatively small and of a similar order to the studies presented above.

CONCLUSIONS

Four different thin-ply, cross-ply carbon composite laminate configurations were designed in order to investigate transverse ply thickness and cracking effects on the fiber direction tensile strain to failure of the material. The coupons were designed with varying thicknesses of 90° plies adjacent to the central 0° plies. A complete set of specimens was tested until failure using video gauge strain and acoustic emission (AE) measurements. Additionally, interrupted tests were conducted and the damage state of the specimens was examined using X-ray computed tomography.

It was found that thin-ply materials are indeed capable of suppressing transverse micro-cracking away from the edges. The developed ex-situ X-Ray CT tests were successfully carried out to determine the extent of damage (edge cracks and matrix cracks) within the configurations. The initiation of edge cracks and their progression into the bulk of the material are distinct mechanisms that should be differentiated. Even though there is local damage present as free-edge cracks, there is not enough energy for these to propagate (Type 1-3 configurations). The Type 4 configuration exhibited extended transverse cracks across the full width of the specimens.

A small drop was found in the failure strain of the Type 1 and Type 2 configurations compared with the baseline which can be attributed to the small edge cracks present. As these cracks further develop across the width of the specimens, a larger volume of the material is affected, hence the further reduction of failure strain due to the load transferred from the 90 plies and stress concentrations at the transverse ply crack tips. Matrix cracking indeed results in reduced fibre direction failure strain, but their overall effect is small.

REFERENCES

1. Christensen, RM. 2017. "Why progress on the failure of fiber composite materials has been so retarded," *J. Reinf. Plast. Compos.* pp. 1–3.
2. Wisnom, M.R. 2013. "The Challenge of Predicting Failure in Composites," in *19th International Conference on Composite Materials*, pp. 12–13. http://www.iccm-central.org/Proceedings/ICCM19proceedings/papers/WIS81754.pdf
3. Czél G., Jalalvand M., and Wisnom M.R. 2016. "Hybrid specimens eliminating stress concentrations in tensile and compressive testing of unidirectional composites," *Compos. Part A Appl. Sci. Manuf.,* 91:436–447.
4. Wisnom M. R., Czél G., Swolfs Y., Jalalvand M., Gorbatikh L., and Verpoest I. 2016. "Hybrid effects in thin ply carbon/glass unidirectional laminates: Accurate experimental determination and prediction," *Compos. Part A Appl. Sci. Manuf.,* 88, pp. 131–139.
5. García I. G., Mantič V., Blázquez A., and París F. 2014. "Transverse crack onset and growth in cross-ply $[0/90]_s$ laminates under tension. Application of a coupled stress and energy criterion," *Int. J. Solids Struct.,* 51, pp. 3844–3856.
6. Rev T. 2020. "Exploiting thin-ply materials to establish controlled failure in carbon composites," *PhD Thesis*, University of Bristol.
7. Camanho P. P., Dávila C. G., Pinho S. T., Iannucci L., and Robinson P. 2006. "Prediction of in situ strengths and matrix cracking in composites under transverse tension and in-plane shear," *Compos. Part A Appl. Sci. Manuf.,* 37, pp. 165–176.
8. ASTM, "ASTM D3039/D3039M - Standard Test Method for Tensile Properties of Polymer Matrix Composite Materials," *Ann. B. ASTM Stand*., pp. 1–13.
9. "Imetrum video gauge system." [Online]. Available: www.imetrum.com
10. Matheson K. E. 2019. Private communication, NASA Langley Research Center.
11. Kohler S., Cugnoni J., Amacher R., and Botsis J. 2019. "Transverse cracking in the bulk and at the free edge of thin-ply composites: Experiments and multiscale modelling," *Compos. Part A Appl. Sci. Manuf.,* 124, pp. 1-13.
12. Xu X., Wisnom M. R., Chang K., and Hallett S. R. 2016. "Unification of strength scaling between unidirectional, quasi-isotropic, and notched carbon/epoxy laminates," *Compos. Part A Appl. Sci. Manuf.,* 90, pp. 296–305.
13. Melnikov A., Swolfs Y., Lomov S. V., and Gorbatikh L. 2018. "Do transverse cracks affect the in-situ strength and fibre breaks accumulation in longitudinal plies of cross-ply laminates?," in *18th European Conference on Composites Materials*.